Cyclohexene Nucleic Acids (CeNA): Serum Stable Oligonucleotides that Activate RNase H and Increase Duplex Stability with Complementary RNA

Jing Wang,[†] Birgit Verbeure,[†] Ingrid Luyten,[‡] Eveline Lescrinier,[†] Matthias Froeyen,[†] Chris Hendrix,[†] Helmut Rosemeyer,[§] Frank Seela,[§] Arthur Van Aerschot,[†] and Piet Herdewijn*[,†]

Contribution from the Laboratory for Medicinal Chemistry, Rega Institute, Minderbroedersstraat 10, B-3000 Leuven, Belgium, Laboratory of Organic Chemistry, Department of Chemistry, Celestijnenlaan 200F, B-3000 Leuven, Belgium, and Laboratorium für Organische und Bioorganische Chemie, Institut für Chemie, Universität Osnabrück, Barbarastrasse 7, D-49069 Osnabrück, Germany

Received January 3, 2000

Abstract: The replacement of the furanose moiety of DNA by a cyclohexene ring gives a new nucleic acid structure: cyclohexene nucleic acids or CeNA. CeNAs can be obtained by the classical phosphoramidite chemisty starting from protected cyclohexenyl nucleoside building blocks. Incorporation of cylcohexenyl nucleosides in a DNA chain increases the stability of a DNA/RNA hybrid. The complex formed between cyclohexenyl oligoadenylate and its DNA or RNA complement is of similar stability. Circular dichroism (CD) and NMR studies indicate easy conformational adaptation of a cyclohexenyl nucleoside when incorporated in a natural nucleic acid structure. CeNA is stable against degradation in serum and a CeNA/RNA hybrid is able to activate E. Coli RNase H, resulting in cleavage of the RNA strand.

Introduction

Replacement of the five-membered furanose ring of natural DNA and RNA with a six-membered ring increases the conformational rigidity of the oligomers.[1] The study of these nucleic acids has contributed considerably to the understanding of the stability and hybridization properties of nucleic acids in general,[2,3] to the etiology of nature's selection of a furanose-based nucleic acids world,[4,5] and to the chiral selection of nucleotides for polymerization reactions.[6] From the structural point of view, these oligonucleotides can be divided in three groups: (a) those with the base moiety positioned at the 1′-position (pyranose nucleic acids); (b) those with the base moiety positioned at the 2′-position (hexitol nucleic acids or HNA); (c) nucleic acids lacking a ring oxygen atom such as cyclohexane nucleic acids (CNA).

β-Pyranose nucleic acids do not hybridize with natural nucleic acids. With HNA, strong self-complementary hybridization and hybridization with natural nucleic acids is observed.[7] CNA also hybridizes with natural nucleic acids and it was suggested that this hybridization is allowed because of a chair flip of the cyclohexane ring in the oligonucleotide structure when compared to its conformation at the monomeric level.[8] A cyclohexane ring usually adopts a chair conformation and chair−chair interconversion is characterized by an activation barrier of ± 12 kcal/mol. Introduction of a double bond into a cyclohexane ring gives a cyclohexene ring with a half-chair form as a global minimum.[9] The cyclohexene system is more flexible than the cyclohexane system, and approaches more the flexibility of a furanose ring. When the two extreme half-chair conformations ($^3H_2$ and $^2H_3$) are compared, it can be concluded that the cyclohexene ring in its $^3H_2$ form is a good mimic of a furanose ring in its C3′-endo conformation[10] (see Supporting Information, S1). In addition, a cyclohexene ring in its $^2H_3$ conformation may be considered as a good mimic of a C2′-endo puckered furanose. Because of this interesting equilibrium, we investigated the incorporation of cyclohexene nucleosides in oligonucleotides and asked (a) if the cyclohexene nucleoside can adopt different conformations when incorporated in a DNA or RNA chain; (b) if the cyclohexene nucleoside can stabilize DNA and/or RNA duplexes; (c) if cyclohexene nucleic acid (CeNA) is stable against nuclease degradation; and (d) whether the modified CeNA/RNA duplex is able to induce RNase H cleavage of the RNA strand.

Results

Synthesis and MS Analysis. For the investigation on the properties of cyclohexene-incorporated nucleic acids, we synthesized the protected phosphoramidite nucleoside with an adenine base moiety. The synthesis of the cyclohexene nucleo-

[†] Laboratory for Medicinal Chemistry, Rega Institute.
[‡] Laboratory of Organic Chemistry, Rega Institute.
[§] Universität Osnabrück.
* To whom correspondence should be addressed. Telephone: +32-16-337387; Fax: +32-16-337340; E-mail: Piet.Herdewijn@rega.kuleuven.ac.be.

(1) Herdewijn, P. *Liebigs Ann. Chem.* **1996**, 1337−1348 and references herein.
(2) Eschenmoser, A. *Pure Applied Chem*. **1993**, *65*, 1179−1188.
(3) Herdewijn, P. *Biochim. Biophys. Acta* **1999**, *19*, 167−179.
(4) Beier, M.; Reck, F.; Wagner, T.; Krishnamurthy, R.; Eschenmoser, A. *Science* **1999**, *283*, 699−703.
(5) Kozlov, I. A.; De Bouvere, B.; Van Aerschot, A.; Herdewijn, P.; Orgel, L. E. *J. Am. Chem. Soc*. **1999**, *121*, 5856−5854.
(6) Kozlov, I. A.; Politis, P. K.; Pitsch, S.; Herdewijn, P.; Orgel, L. E. *J. Am. Chem. Soc*. **1999**, *121*, 1108−1109.
(7) Hendrix, C.; Rosemeyer, H.; De Bouvere, B.; Van Aerschot, A.; Seela, F.; Herdewijn, P. *Chem. Eur. J.* **1997**, *3*, 1513−1520.
(8) Maurinsh, Y.; Rosemeyer, H.; Esnouf, R.; Medvedovici, A.; Wang, J.; Ceulemans, G.; Lescrinier, E.; Hendrix, C.; Busson, R.; Sandra, P.; Seela, F.; Van Aerschot, A.; Herdewijn, P. *Chem. Eur. J*. **1999**, *5*, 2139−2150.
(9) Cremer, D.; Szabo, K. J. In *Conformational Behaviour of Six-membered Rings*; Juaristi, E., Ed.; VCH Publishers: New York, 1995; pp 113−117.
(10) Wang, J.; Herdewijn, P. *J. Org. Chem.* **1999**, *64*, 7820−7827.

10.1021/ja000018+ CCC: $19.00
Published on Web 08/23/2000

Scheme 1. Synthesis of the Phosphoramidite Building Block of 9-[(1*S*,4*R*,5*S*)-5-hydroxy-4-hydroxymethyl-2-cyclohexenyl]adenine (A_1) and Structure of Anhydrohexitol-A (A_2)

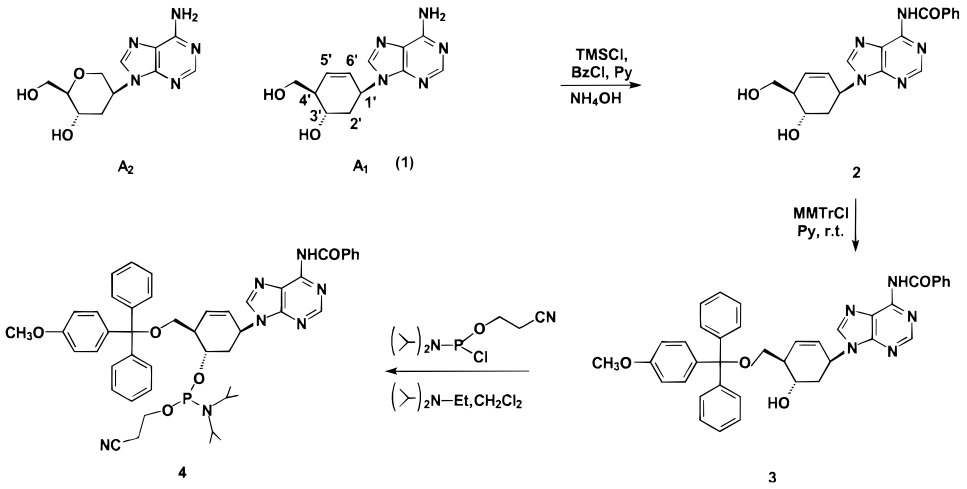

side itself is described separately.[10] The adenine base moiety was protected with a benzoyl group and the primary hydroxyl group was protected with a monomethoxytrityl group (Scheme 1). The secondary hydroxyl group was reacted with 2-cyanoethyl-*N*,*N*-diisopropyl-chlorophosphoramidite to yield the nucleotide building block. Assembly of the monomers into oligonucleotides was done as described previously.[8] The carbocyclic analogue was used at 0.12 M and coupling was allowed to proceed for 3 min, resulting in highly efficient coupling (>95%). Total isolated yield—following ion exchange and desalting by gel penetration—for approximately a 1 μmol scale synthesis amounted to 61 OD_{260} (31% overall yield) compared with 56 OD (29% overall) for the analogous HNA sequence and 62 OD (32% overall) for a natural $(dA)_{13}$ sequence. Crude ion exchange profiles more adequately reflect the synthesis quality, and this is exemplified by the ion exchange profile of the crude mixture for the fully modified $(A_1)_{13}$ sequence where only a few failure sequences could be detected (see Supporting Information, S2).

During assembly of the first oligos, the excess of amidite used was collected and hydrolyzed to the H-phosphonate, after which the phosphonate moiety was cleaved using a recent procedure of Jones,[11] which allowed recycling of the phosphoramidite **4**. As proof of correct incorporation of the cyclohexenyl building block, the modified oligonucleotide [5′-d(CGC GAA$_1$TTCGCG-3′)] was desalted by cation exchange beads and analyzed by mass spectrometry. The electrospray ionization (ESI)−MS spectrum showed several peaks corresponding to multiply charged ions of the sample in the charge states $[M-3H]^{3-}$ to $[M-6H]^{6-}$. The deconvoluted spectrum, calculated by Max Ent 1 processing, indicates the experimental monoisotopic mass to be 3654.71 Da, confirming the identity of the oligonucleotide (calculated 3654.74 Da). Further MS−MS analysis of the $[M-4H]^{4-}$ peak at 912.68 Da allowed several fragment peaks to be assigned. All other sequences containing the cyclohexene adenosine analogue likewise were analyzed via ESI−MS (Table 1).

Hybridization Properties of Oligonucleotides with Cyclohexenyl-Modified Nucleosides Incorporated. To test the influence of a cyclohexenyl nucleoside on the stability of dsDNA, DNA/RNA, and dsRNA sequences, we incorporated cyclohexenyl-A (Scheme 1, A_1) in a mixed purine−pyrimidine DNA sequence (5′-CCAGTGATATGC-3′) and in the same RNA sequence (5′-CCAGUGAUAUGC-3′). The influence of the cyclohexenyl nucleoside on duplex stability was compared with that of an anhydrohexitol nucleoside (Scheme 1, A_2). In both cases one, two, and three natural adenine nucleosides were replaced by the unnatural A_1 or A_2. The incorporation of cyclohexenyl-A (A_1) results only in a small decrease of the stability of dsDNA (Table 2) A ΔT_m/mod of −0.5 °C was observed, independent of whether one, two, or three modified nucleosides were incorporated. A similar decline in stability was found after incorporation of anhydrohexitol-A (A_2). The influence of A_1 and A_2 on the duplex stability of dsDNA does not seem to be fundamentally different.

Of more interest is the influence of cyclohexenyl-A on the stability of a DNA/RNA duplex. Incorporation of one, two, or three cyclohexenyl-A nucleosides in the DNA strand increases duplex stability with +1.1, +1.6, and +5.2 °C respectively, which means a ΔT_m/mod of +1.1, +0.8, and +1.7 °C. As expected, the influence on duplex stability is dependent on the

Table 1. ESI−MS Data (Average Mass) of A_1 Comprising Oligonucleotides

sequence	calcd.	found
5′-CCA$_1$GTGA$_1$TA$_1$TGC	3675.5	3675.1
5′-CCAGTGA$_1$TA$_1$TGC	3665.5	3665.1
5′-CCAGTGA$_1$TATGC	3655.5	3655.1
5′-r(CCA$_1$GTGA$_1$TA$_1$TGC	3777.4	3777.0
5′-CGCGAA$_1$TTCGCG	3654.7	3654.7
5′-$(A_1)_{13}$-propanediol	4278.3	4278.1

Table 2. Influence of the Incorporation of A_1 and A_2 on the Stability of DsDNA, DsRNA and DNA/RNA Duplexes

	DNA complement		RNA complement	
DNA sequence	T_m (°C)	ΔT_m/mod (°C)	T_m (°C)	ΔT_m/mod (°C)
5′-CCAGTGATATGC-3′	49.8		44.0	
5′-CCAGTGA$_1$TATGC-3′	49.4	−0.4	45.1	+1.1
5′-CCAGTGA$_1$TA$_1$TGC-3′	48.5	−0.6	45.6	+0.8
5′-CCA$_1$GTGA$_1$TA$_1$TGC-3′	48.1	−0.6	49.2	+1.7
5′-CCAGTGA$_2$TATGC-3′	49.5	−0.3	46.9	+2.9
5′-CCAGTGA$_2$TA$_2$TGC-3′	49.3	−0.2	48.7	+2.3
5′-CCA$_2$GTGA$_2$TA$_2$TGC-3′	47.5	−0.8	53.1	+3.0
5′-$(dA)_{13}$−3′	33.1		15.2	
6′-$(A_1)_{13}$−4′	33.5	0.0	34.2	+ 1.4
6′-$(A_2)_{13}$-4′	23.3	−0.75	32.9	+ 1.3
RNA sequence				
5′-CCAGUGAUAUGC-3′	49.1		58.3	
5′-CCA$_1$CUGA$_1$UA$_1$UGC-3′	47.6	−0.5	58.9	+ 0.2

(11) Song, Q.; Wang, W.; Fischer, A.; Zhang, X.; Gaffney, B. L.; Jones, R. A. *Tetrahedron Lett.* **1999**, *40*, 4153−4156.

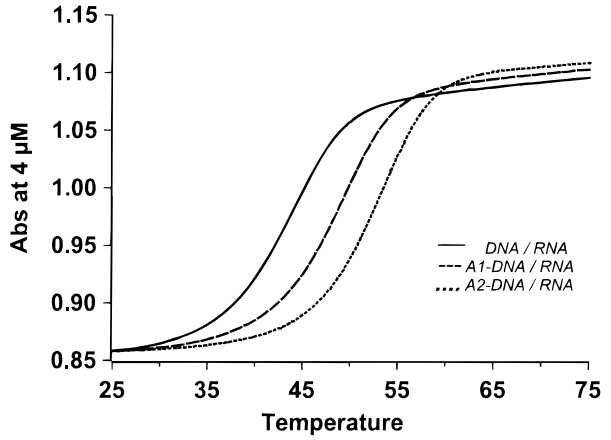

Figure 1. T_m curves for DNA/RNA hybrids before and after incorporation of, respectively, A_1 or A_2 in the DNA strand: DNA, 5′-CCAGTGATATGC-3′; A_1-DNA, 5′-CCA$_1$GTGA$_1$TA$_1$TGC-3′; A_2-DNA, 5′-CCA$_2$GTGA$_2$TA$_2$TGC-3′; RNA, 5′-GCAUAUCACUGG-3′.

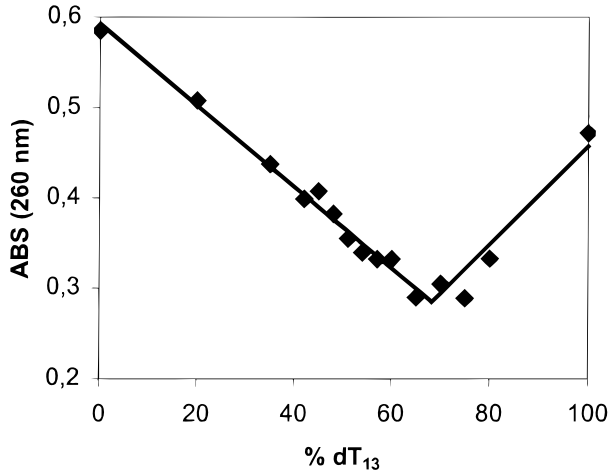

Figure 2. UV mixing curves of $(A_1)_{13}$ and dT_{13}. The experiment was carried out at pH 7.5 in 0.1 M NaCl.

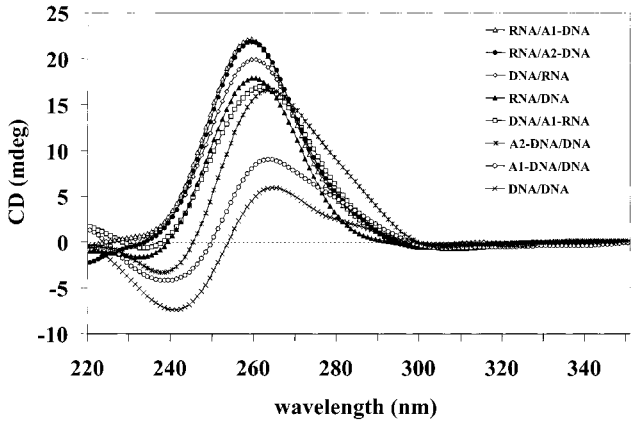

Figure 3. CD spectra of dsDNA before and after incorporation of A_1 and A_2 in one of the DNA strands. DNA, 5′-GCA TAT CAC TGG-3′; A_1-DNA, 5′-CCA$_1$ GTGA$_1$ TA$_1$ TGC-3′; A_2-DNA, 5′-CCA$_2$ GTGA$_2$ TA$_2$ TGC-3′; and CD spectra of DNA/RNA complexes before and after incorporation of A_1 and A_2 in the DNA strand. DNA/RNA, d(5′-GCA TAT CAC TGG-3′)/r(5′-CCA GUG AUA UGC-3′); RNA/DNA, r(5′-GCA UAU CAC UGC-3′)/d(5′-CCA GTG ATA TGC-3′); for A_1-DNA and A_2-DNA, see Scheme 1.

incorporation site of A_1. The stabilization effect of A_2 on the DNA/RNA duplex is twice as high as that of A_1; the sequence selective effect is the same. An overlay of the melting curves for DNA/RNA duplexes with a triple substitution of A_1 or A_2, respectively, is depicted in Figure 1. When cyclohexenyl-A is incorporated in the RNA strand of a DNA/RNA duplex, a ΔT_m/mod of −0.5 °C is observed (Table 2). Note that the difference in stability of the DNA/RNA complex and the RNA/DNA complex is 5 °C. Incorporation of three residues of A_1 in a dsRNA sequence leads to an increase in duplex stability of +0.6 °C. The increase in duplex stability after incorporation of A_1, using RNA as the complementary strand, suggests that the conformation of A_1 in the duplex may be related to the 3′-endo conformation of the ribofuranose sugar. The $^3H_2$ conformation of A_1 is indeed the most stable conformation of cyclohexenyl-A and conformational preorganization may be the basis of this duplex stabilization.

The reason for the small decrease in stabilization of a dsDNA duplex, after incorporation of A_1, is less clear. Several hypotheses may be formulated. Cyclohexenyl-A may adopt the $^2H_3$ conformation when incorporated in a dsDNA sequence (which is a mimic of a furanose nucleoside in its 2′-endo conformation). However, this conformation is of higher energy than the $^3H_2$ conformation and this is reflected in a lower duplex stability. Another explanation might be that cyclohexenyl-A adopts a $^3H_2$ conformation when incorporated in dsDNA and that this conformation is less well accommodated in the dsDNA duplex, leading to local duplex distortion.

Although the nature of the oligoadenylate−oligothymidylate associations deviates from the structure of the complexes formed between mixed-base oligomers, the study of this complex may give us a good idea about the potential of a modified nucleic acid to undergo conformational changes. The complex formed between cyclohexenyl oligoadenylate and poly(U) has similar stability to that between anhydrohexitol oligoadenylate and poly(U). However, of interest is the observation that the cyclohexenyl oligoadenylate−poly(dT) complex is much more stable (ΔT_m: +10 °C) than the corresponding anhydrohexitol oligoadenylate−poly(dT) complex. The nature of the cyclohexenyl oligoadenylate−poly(dT) complex was determined by a titration experiment (Figure 2) and found to be of triplex origin [$(dT)_{13}$·$(A_1)_{13}$·$(dT)_{13}$]. The complex formed between cyclohexenyl oligoadenylate and its DNA (poly(dT)) or RNA (poly(U)) complement is of similar stability. These results may indicate that CeNAs are flexible molecules and that cyclohexene nucleotides can be accommodated in different kinds of complexes.

Structural Investigations of CeNA-Containing Complexes Using CD Spectral Analysis. CD spectral analysis may give us a first idea whether incorporation of cyclohexenyl-A has a fundamental influence on the conformation of a double-helical structure. Therefore, a comparison was made between the CD spectra of the duplexes containing three A_1 residues, the natural reference duplexes, and the same complexes having three A_2 residues incorporated. Because of its particular structure, which is not very relevant for the antisense work, we prefer not to study the oligoadenylate systems. Moreover, it was demonstrated that oligo(A_1) and oligo(dT) form a complex in a 1:2 ratio. The CD spectra of the dsDNA sequences (Figure 3) are characterized by a positive cotton effect at 264 nm and a negative cotton effect at 241 nm. After incorporation of three A_1 residues (A_1−DNA/DNA), the spectrum is similar but not the same. The positive CD band at 264 nm is more intense while the negative CD band at 238 nm is less intense. This trend continues when three A_2 residues are incorporated (A_2−DNA/DNA). The negative signal at 238 nm becomes weaker while the intensity of the positive band at 264 nm increases. The spectrum of the A_2−DNA/DNA complex becomes more similar to the DNA/RNA duplex while

the spectrum of the A_1−DNA/DNA complex is intermediate between that of a DNA/DNA and RNA/DNA duplex. This is a first indication that the structures of A_1−DNA/DNA and A_2−DNA/DNA are different. The CD spectra of the complexes RNA/A_1−DNA; RNA/A_2−DNA; DNA/RNA; RNA/DNA; and DNA/A_1−RNA are very similar (Figure 3). An intense positive CD band is observed around 260 nm while nearly no (or bands of very low intensity) negative signals are present. The intensity of the positive band decreases in the order given. All complexes seem to have the same general geometry. The same can be said about the spectra of the dsRNA and RNA/A_1−RNA complexes (spectra not shown), although the positive band is somewhat shifted to shorter wavelength. The CD spectral analyses demonstrate similar conformation for all RNA-containing complexes. Three A_2 residues incorporated in a DNA chain seem to induce a conformational change of a dsDNA duplex in the direction of a DNA/RNA type structure. Three A_1 residues do not seem to have this effect and the DNA/A_1−DNA conformation stays close to the typical dsDNA form. This might be explained by a different conformation of cyclohexenyl-A in a dsDNA and in a DNA/RNA duplex. Conformational changes (chair inversion) of A_2 cost a lot of energy, whereas A_1 is expected to undergo more easily half-chair inversion.

Structural Investigation of the Dickerson Dodecamer Containing a Cyclohexenyl-A Residue (A_1) Using NMR Spectroscopy and a Computer Model. To study the effect of incorporation of cyclohexenyl-A on the conformation of a DNA duplex in more detail we incorporated one D-cyclohexenyl-A (A_1) residue in the well-known self-complementary Dickerson dodecamer, 5′-d[CGCGAA$_1$TTCGCG]$_2$-3′ (**I**), and investigated the solution state conformation using NMR. Under the appropriate experimental conditions (1.4 mM oligomer, 10 mM KH_2PO_4, 10 μM ethylenediaminetetraacetic acid (EDTA), pH 7.5 in 90% H_2O/10% D_2O), the imino protons of guanine and thymine give rise to NMR peaks in the range of 12−14 ppm in a 1D WATERGATE spectrum.[12] The imino protons of neighboring base-pairs in a base-paired helical region are close enough to give nuclear Overhauser effect (NOE) cross-peaks in a 2D spectrum and these imino−imino NOE cross-peaks between the neighboring base-pairs are clearly seen in the 2D WATERGATE nuclear Overhauser enhancement spectroscopy (NOESY) spectrum. The NOE connectivity walks on the 2D spectrum (spectra not shown) and the sequential imino proton assignments correspond with a symmetric duplex. NOEs for the adenine H2 (AH2) of the A−T base-pairs to their own T imino proton and to the imino protons of neighboring pairs also prove the presence of a duplex. Nonexchangeable proton assignments are based on an analysis of through-space NOESY,[13] through-bond (correlation spectroscopy (COSY),[14] total correlation spectroscopy (TOCSY)[15] and ^{1}H-^{31}P heteronuclear correlation (HETCOR)[16] datasets using well-described procedures for DNA duplexes.[17] Figure 4b shows a fragment of a NOESY spectrum (250 ms) of the duplex (**I**) at 20 °C in D_2O showing cross-peaks between the base protons (H6 in pyrimidines or H8/H2 in purines) and anomeric protons and pyrimidine H5 protons; the spectrum was used to assign base (H8/H6/H2) and H1′ protons in a sequential manner. Table 3 contains the aromatic and H1′ proton chemical shifts of the modified duplex (**I**) at 20 and 25 °C and of the unmodified duplex (**II**) 5′-d[CGCGAATTCGCG]$_2$-3′.[18,19] Chemical shift changes are indicative of structural changes associated with the introduction of modified nucleotides. Table 3, however, shows negligible changes in chemical shift (max 0.1 ppm difference) for all the other residues, implying that A_1 does not disturb the B-structure of the duplex. The changes are limited to the modified nucleotide itself. Figure 5 shows a NOESY−COSY connectivity diagram for sequential assignments via a NOESY spectrum (50 ms) between base protons and 2′C protons using NOESY with a mixing time of 50 ms and a double quantum filtered COSY spectrum which contains the cross-peaks between 1′ H and 2′-CH_2. The observations that (i) most of the H2″ protons are more downfield in chemical shift than are the H2′ protons; (ii) the intraresidue and interresidue NOES between H8/H6 and H2′ and H2″, respectively, are more intense than the intraresidue NOES between H8/H6 and H2″; and (iii) the H1′−H2′, H1′−H2″ cross-peaks have characteristic B-like phase-sensitive multiplets, confirms as well the existence of a regular B-type DNA structure.

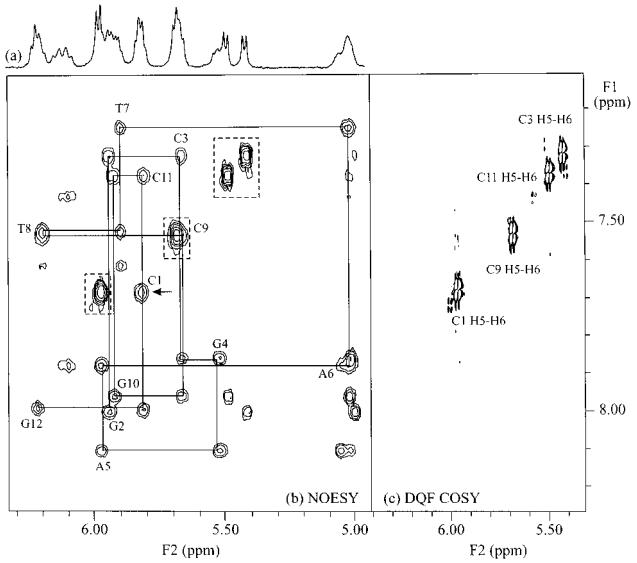

Figure 4. (a) 1D H1′ and H5 proton region of (I). (b) (H8/H6/H2)−H1′/H5 region of the 250 ms NOESY of (**I**) at 20 °C in 100% D_2O. Sequential H8/H6$_{(n)}$−H1′$_{(n)}$−H8/H6$_{(n+1)}$ connectivities starting from the 5′ end (C1) (labeled by arrow) are shown in solid lines. Resonances at 7.42 and 7.61 ppm are from A5H2 and A6H2, respectively. (c) H5−H6 region of the DQF COSY of (**I**) at 20 °C in 100% D_2O.

However, the NOESY spectrum (Figure 4b) and the DQF COSY spectrum (Figure 4c), representing the region of cross-peaks between the base protons (H6/H8) and anomeric protons (H1′) and between H5 and H6 protons of the pyrimidine residues and the H1′/H5 proton region of the 1D spectrum (Figure 4a), show the presence of broad proton cross-peaks and multiple resonances (some of them are boxed by dashed lines in Figure 4b), suggesting the presence of multiple species. No peak sharpening is observed by varying the temperature over the range of 25 to 45 °C, or by changing the salt concentration. A more detailed structural analysis is in progress. Initial results

(12) Piotto, M.; Saudek, V.; Sklenar, V. *J. Biomol. NMR* **1992**, *2*, 661−665.
(13) Jeener, J.; Meier, B. H.; Bachman, P.; Ernst, R. R. *J. Chem. Phys.* **1979**, *71*, 4546−4553.
(14) Rance, M.; Sørensen, O. W.; Bodenhausen, G.; Wagner, G.; Ernst, R. R.; Wütrich, K. *Biochem. Biophys. Res. Commun.* **1983**, *117*, 479−485.
(15) Griesinger, C.; Otting, G.; Wütrich, K. *J. Am. Chem. Soc.* **1988**, *110*, 7870−7872.
(16) Sklenar, V.; Miyashiro, H.; Zon, G.; Miles, H. T.; Bax, A. *FEBS Lett.* **1986**, *208*, 94−98.
(17) Wijmenga, S. S.; Mooren, M. W.; Hilbers, C. W. In *NMR of Macromolecules. A Practical Approach*; Roberts, G., Ed.; Oxford University Press: New York, 1993, pp 217−288.
(18) Yamakage, S.-I.; Maltseva, T. V.; Nilson, F. P.; Földesi, A.; Chattopadhyaya, J. *Nucleic Acids Res.* **1993**, *21*, 5005−5011.
(19) Marathias, V. M.; Sawicki, M. J.; Bolton, P. H. *Nucleic Acids Res.* **1999**, *27*, 2860−2867.

Table 3. Chemical Shifts (ppm) of the Modified Duplex (**I**) for the Aromatic and Anomeric Protons Compared with Those of the Dickerson Duplex (**II**) Published in Literature[23,24]

	H8/H6				H1'			
residue *z*	(**II**)[23] at 15 °C	(**I**) at 20 °C	(**I**) at 25 °C	(**II**)[24] at 21 °C	(**II**)[23] at 15 °C	(**I**) at 20 °C	(**I**) at 25 °C	(**II**)[24] at 21 °C
C1	7.75	7.68	7.69	7.72	5.81	5.81	5.82	5.84
G2	8.16	8.00	8.00	8.04	5.97	5.93	5.93	5.98
C3	7.46	7.32	7.33	7.36	5.61	5.66	5.68	5.68
G4	8.07	7.85	7.86	7.95	5.55	5.53	5.52	5.53
A5	8.30	8.10	8.11	8.20	6.08	5.96	5.97	6.09
$A_1$6/A6	8.31	7.87	7.87	8.21	6.21	5.04	5.04	6.25
T7	7.36	7.24	7.26	7.20	6.01	5.89	5.90	6.00
T8	7.56	7.52	7.53	7.46	6.19	6.19	6.19	6.19
C9	7.64	7.53	7.54	7.56	5.79	5.67	5.67	5.75
G10	8.10	7.96	7.95	8.00	5.92	5.91	5.91	5.94
C11	7.54	7.37	7.38	7.42	5.80	5.80	5.82	5.84
G12	8.15	7.99	7.99	8.03	6.24	6.20	6.20	6.24

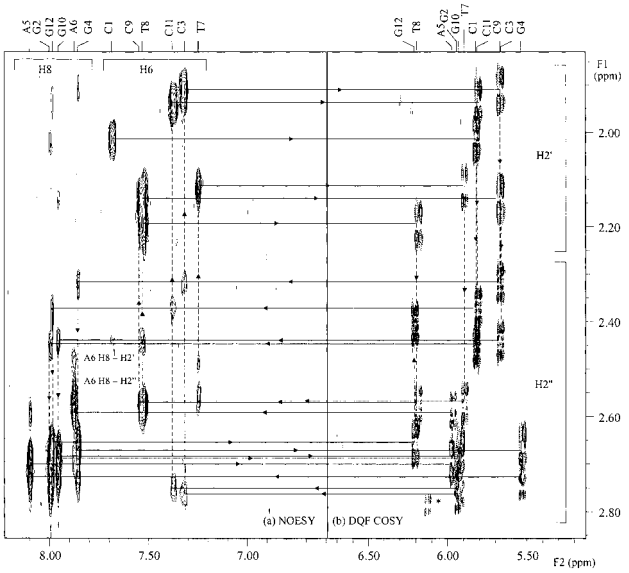

Figure 5. NOESY−COSY connectivity diagram for sequential assignments via NOEs between base protons and the 2′C protons using NOESY with a mixing time of 50 ms and DQF−COSY representing the region of the H1′−H2′/H2″ cross-peaks. In the NOESY spectrum (a), successive cross-peaks $d_s(2'';6,8)$ and $d_i(6,8;2')$ are connected by dashed vertical lines. In the COSY spectrum (b) the cross-peaks H1′−H2′ and H1′−H2″ of each nucleotide are connected by dashed vertical lines. Horizontal lines connect the cross-peaks $d_i(6,8;2')$ with H1′−H2′ cross-peaks of the same nucleotide and the H1′−H2″ cross-peaks are connected with the cross-peaks $d_s(2'';6,8)$. The arrows indicate where the sequential assignment can be followed from C1 to G12. Sequence-specific assignments for the base protons and the H1′ protons are indicated at the top. The cross-peaks indicated with the asterisk represent the H4′−H5′/H6′ cross-peaks.

indicate that the incorporation of the cyclohexenyl-A residue (A_1) has practically no effect on the global structure of the Dickerson dodecamer and changes manifest themselves only at the modified sixth residue (A_1) and its direct neighboring residues. However, the line broadening and multiple resonances suggest that the cyclohexenyl-A (A_1) residue induces conformational mobility.

The experimental results (CD spectral analysis) suggest that A_1 can be accommodated as well in a dsDNA as in a dsRNA duplex. NMR measurement confirms the conformational mobility of a cyclohexene nucleoside when incorporated in an oligonucleotide. We assume that a cyclohexene nucleoside adopts a $^3H_2$ conformation in the A-type CeNA/RNA duplex and a $^2H_3$ conformation in the B-type CeNA/DNA duplex. The nucleoside in the $^2H_3$ conformation is only 1.64 kJ/mol more stable than that in the $^3H_2$ conformation.

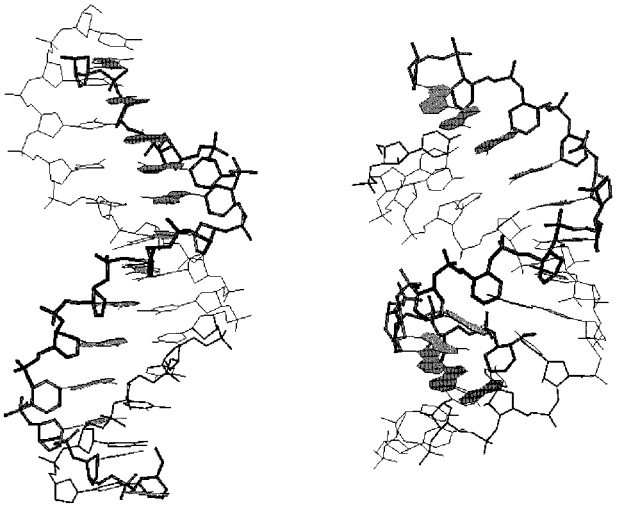

Figure 6. Model structures of CeNA oligonucleotides with complementary DNA (left) and RNA (right). The pictures are snapshots from a 100 ps molecular dynamics simulation with explicit water solvent. The phosphate−sugar backbone of CeNA is highlighted as sticks. The initial CeNA/DNA duplex has been built from an idealized right-handed Arnott B-type double helix (12 A/T base pairs) with the CeNA sugars in the $^2H_3$ conformation (Figure 1, left) where the base is oriented pseudoequatorially. The CeNA/RNA duplex is generated starting from an idealized right-handed Arnott A-type double helix (12 A/U base pairs) with the CeNA sugars in the $^3H_2$ conformation (Figure 1, right), orienting the adenine base in the pseudoaxial position.

To evaluate the potential of CeNA for conformational adaptation, a model structure was built of CeNA/RNA [$(A_1)_{13}$/$(rU)_{13}$] and of CeNa/DNA [$(A_1)_{13}$/$(dT)_{13}$]. Despite the experimental evidence that the complex with DNA exists as a triplet, the second (duplex) model was investigated because of reasons of simplicity. The stability of the models was investigated using short molecular dynamics (MD) simulations (Figure 6). During the MD simulation both helical structures are stable. The CeNA residues stay in their initial conformation ($^3H_2$ in RNA complex and $^2H_3$ in the DNA complex). The interhelical hydrogen bond pattern is conserved except at the end residues, where in the case of the A-helix, the inter-base hydrogen bonds are frequently broken and restored.

Serum Stability of CeNA and Cleavage of CeNA/RNA Hybrids by *Escherichia coli* RNase H. Because only the cyclohexenyl-A nucleotide is currently available, we used a double chimeric approach to evaluate the RNase H susceptibility of the CeNA/RNA duplex (Figure 7). Therefore, we synthesized a chimeric 2′-*O*-methyl RNA/RNA oligonucleotide that is complementary to the chimeric DNA/CeNA oligonucleotide (see

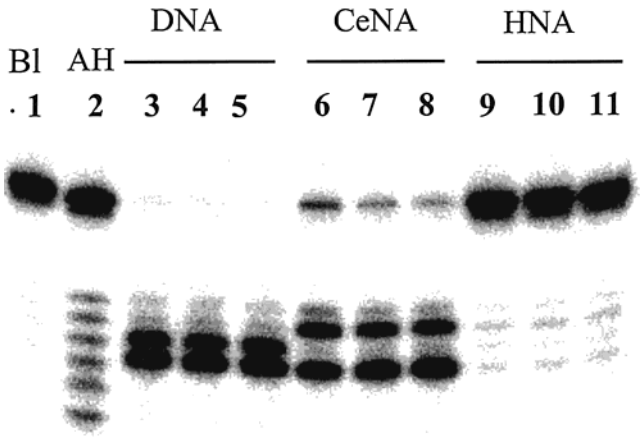

Figure 7. RNase H-mediated hydrolysis of chimeric 2′-*O*-methyl RNA−RNA oligonucleotide 5′-m(CGGCG)r(U)$_6$ m(CAGGA)-3′ upon hybridization with a complementary sequence 5′-d(TCCTG) (X)$_6$ d(CGCCG) where X = dA, A_1 or A_2, respectively. lane 1, RNA target; lane 2, partial alkaline hydrolysis (0.2 M Na_2CO_3, 80 °C, 5 min) of RNA target; lanes 3−5, RNase H activity toward DNA/RNA duplex (incubation times 1, 3, and 6h); lanes 6−8, RNase H activity toward CeNA/RNA duplex (incubation times 1, 3, and 6h); lanes 9−11, RNase H activity toward HNA/RNA duplex (incubation times 1, 3, and 6h).

legend Figure 7). We did not use a full RNA oligonucleotide as complement of the DNA/CeNA chimer because strand cleavage may then occur outside the CeNA/RNA region. It has been reported that 2′-*O*-methyl RNA/DNA hybrids are not substrates for RNase H[20] and that partially modified chimeric oligonucleotides containing deoxy gaps of five residues or longer could activate RNase H in vitro, although less efficiently than the parent uniform deoxynucleotide.[21] The use of fully modified poly A sequences should also be avoided because experimentally it was observed that oligoadenylate−poly(rU) complexes [(dA)$_{13}$/poly(rU) and (A$_1$)$_{13}$/poly(rU)] are poor substrate for RNase H of *E. coli* (data not shown). For the study of cleavage of the rU strand by RNase H, a chimeric oligo(rU)/oligo(dA) duplex was used as positive control (Figure 7, lane 3) and an oligo(rU)/oligo(A$_2$) was used as negative control[7] (Figure 7, lane 5). *E. coli* enzyme was used for the study of the susceptibility of the hybrids to be cleaved by RNase H because this enzyme is readily available and its cleavage properties are not very different from those of the mammalian enzyme.[21]

Figure 7 shows the cleavage pattern of the three complexes after incubation, respectively, for 1, 3, and 6 h with *E. coli* RNase H. The DNA/RNA complex is quickly degraded (lane 3), while the HNA-containing complex (lane 5) is not degraded at all. The complex formed between the cyclohexenyl oligomer and its RNA complement is an efficient substrate for RNase H. Two cleavage sites in the RNA strand are observed for the latter complex, i.e., one between (U)$_7$ and (U)$_8$ and the other between (U)$_9$ and (U)$_{10}$. The cleavage pattern in an oligo(rU) sequence is dependent on the sugar modification in the complementary A-tract. Indeed, the DNA/RNA complex is not only degraded faster, but cleavage occurs preferentially between (U)$_8$ and (U)$_9$ and between (U)$_9$ and (U)$_{10}$. Displacement of A_2 by the conformationally more mobile A_1 results in a large difference in cleavage susceptibility.

The stability of the modified oligonucleotide was likewise tested in serum (see Supporting Information, S3). This experiment proved that CeNA has serum stability similar to that of HNA. Both modified oligonucleotides are much more stable against enzymatic degradation (no degradation after incubation for 3 h in serum 37 °C) than DNA (almost half degraded after 3 h incubation). CeNA combines the interesting future of serum stability and the properties to induce RNase H.

Discussion

An ideal antisense oligonucleotide is considered to be an oligomer hybridizing strongly with its RNA complement and able to induce RNase H-cleavage of the target.[23] The development of such a molecule is a difficult undertaking because both properties are difficult to combine in one construct. Strong hybridization of charged nucleic acids to RNA means preorganization in an A-type duplex for maximal interstrand stacking. The more the nucleoside building block is preorganized in an N-type furanose conformer, the higher the stability of the duplex formed between the modified oligomer and its RNA complement.[1,3] However, the minor groove width of stable A-type duplexes is too large for efficient recognition by RNase H.[22,24] The minor groove of an RNA/DNA hybrid is narrower than that of A-form duplexes (dsRNA) but wider than that of B-form (dsDNA) duplexes.[22] In an RNA/DNA duplex, the ribose moieties of the RNA strand have a N-conformation whereas the deoxyribose moieties of the DNA strand deviate from the typical S-conformation. It seems, therefore, that a compromise between both might be the best solution for antisense purposes and that a rather modest increase in duplex stabilization (based on a preorganization in, for example, an O4′-endo conformation)[22] might be compatible with RNase H activation. RNase H is activated by RNA/DNA hybrids in which the DNA strand represents phosphodiester or phosphorothioate oligonucleotides.[25] The latter oligomers have a modified "phosphate" internucleoside linkage. As far as we know, the only sugar-modified oligonucleotides that activate (*E. coli*) RNase H are arabinonucleic acids with either a 2′-hydroxyl- or a 2′-fluoro substituent.[26] Oligo-arabinonucleic acids (2′-OH) destabilize the RNA/DNA duplex considerably and have no advantage over phosphorothioate oligonucleotides.[26] Duplexes between 2′-deoxy-2′-fluoro-β-D-arabinonucleic acids and RNA are more stable than DNA/RNA hybrids (an average ΔT_m/mod of +0.27 °C for poly (A/T) and +0.77 °C for a mixed sequence) and they are prime candidates to be evaluated as antisense molecules in a cellular system. In relationship to the structural requirements for RNase H susceptibility, the observation of Berger et al. that the 2′-deoxy-2′-fluoro-arabinofuranosyl ring adopts a O4′-endo conformation when incorporated in the Dickerson−Drew double-stranded DNA dodecamer, is remarkable.[27] The CeNAs described in this manuscript are composed of flexible cyclohexene nucleotides. We calculated that the energy difference between both conformations (for a purine nucleoside) is about 1.6 kJ/mol and that the half-chair conformation with the base in a pseudoaxial position ($^3H_2$) is preferred.[10] The low energy

(20) Inoue, H.; Hayase, Y.; Iwai, S.; Ohtsuka, E. *FEBS Lett*. **1987**, *215*, 327−330.
(21) Monia, B. P.; Lesnik, E. A.; Gonzalez, C.; Lima, W. F.; McGee, D.; Guinosso, C. J.; Kawasasaki, A. M.; Cook, P. D.; Freier, S. M. *J. Biol. Chem*. **1993**, *268*, 14514−14522.
(22) Fedoroff, O. Y.; Salazar, M.; Reid, B. R. *J. Mol. Biol*. **1993**, *233*, 509−523.
(23) Crook, S. T. *Antisense Nucl. Acid Drug Devel*. **1999**, *9*, 377−379.
(24) Gyi, J. I.; Conn, G. L.; Lane, A. N.; Brown, T. *Biochemistry* **1996**, *35*, 12538−12548.
(25) Stein, C. A.; Subasinghe, C.; Shinozuka, K.; Cohen, J. S. *Nucleic Acids Res*. **1988**, *16*, 3209−3221.
(26) Damha, M. J.; Wilds, C. J.; Noronha, A.; Brukner, I.; Borkow, G.; Arion, D.; Parniak, M. A. *J. Am. Chem. Soc*. **1998**, *20*, 12976−12977.
(27) Berger, I.; Tereshko, V.; Ikeda, H.; Marquez, V. E.; Egli, M. *Nucleic Acids Res*. **1998**, *26*, 2473−2480.

difference between both conformers can be explained by the stabilization of the $^3H_2$ form via $\pi-\sigma^*$ interactions, while the $^2H_3$ is sterically less demanding. When incorporated in a DNA sequence, the CeNA residues increase the stability of the duplex formed between this DNA and its complementary RNA. For the sequence studied, the ΔT_m/mod averages +1.2 °C. The capacity of a cyclohexene nucleotide to undergo conformational changes and to be accommodated in different nucleic acid structures was evaluated at three different levels. The complex between CeNA (oligo A) and DNA (oligo dT) is of triple helical origin and has a stability similar to the complex between CeNA (oligo A) and RNA (oligo rU) (which is not the case for HNA/DNA and HNA/RNA). Second, the CD spectrum of an A_1−DNA/DNA duplex is similar to the spectrum of dsDNA (which is not the case for a A_2−DNA/DNA duplex). The CD spectrum of an RNA/A_1−DNA duplex is similar to the spectrum of RNA/DNA and the CD spectra of RNA/A_1−RNA and of dsRNA are identical. Third, NMR analysis of a Dickerson dodecamer containing A_1 suggest conformational mobility of this residue.

The CeNA when hybridized to RNA is, likewise, able to activate RNase H. In contrast, the HNA/RNA duplex is not degraded. It might be expected that the minor groove width of the CeNA/RNA duplex is comparable to that of a DNA/RNA duplex (9 Å) and that RNase H can efficiently bind to the complex. dsRNA with a minor groove width of 11 Å is not degraded at all. CeNA/RNA duplexes have a similar flexibility to that of DNA/RNA duplexes,[24] with the advantage that the CeNA/RNA duplexes are thermally more stable than the natural counterparts and that CeNA is stable against degradation in serum.

Summary

In pyranose nucleic acids, the nucleobase is equatorially oriented both at the level of the monomer and at the oligonucleotide level. These oligomers form strong self-complementary duplexes, in case hybridization is not hindered for steric reasons.[28] The oligomers do not hybridize with natural nucleic acids. The hexitol nucleic acids have axially oriented nucleobases at the level of the monomer as well as at the level of the oligomer. They hybridize strongly and selectively with RNA, which is explained by the similarities between the hexitol ring and a furanose ring frozen in its 3′-endo conformation.[29] The cyclohexane nucleosides may adopt two chair conformations, one with axially oriented base moieties which is preferred for hybridization of cyclohexane nucleic acids with natural nucleic acids, and one with equatorially oriented bases (resembling the pyranose nucleic acids situation).[8] Here, we demonstrated that CeNAs are much more flexible than the previously synthesized six-membered nucleic acids. The structural similarity between a cyclohexene nucleoside and a natural furanose nucleoside is reflected in the observation that CeNAs can undergo conformation changes similar to those of natural nucleic acids. CeNA can be considered as a new oligonucleotide combining the advantage of duplex stabilization and serum stability with the potential to activate RNase H, which means that these oligomers are prime candidates for evaluation as antisense constructs in a cellular system.

Experimental Section

Ultraviolet spectra were recorded with a Philips PU8740 UV/Vis spectrophotometer. The ^{1}H NMR and ^{13}C NMR spectra were recorded with a Varian Gemini 200 spectrometer. Tetramethylsilane (TMS) was used as internal standard for the ^{1}H NMR spectra (s = singlet, d = doublet, t = triplet, m = multiplet), $CDCl_3$ (δ = 76.9) or CD_3OD (δ = 49.0) for the ^{13}C NMR spectra. Mass spectrometry measurements were obtained using a Kratos Concept 1H mass spectrometer. Pyridine was refluxed overnight on potassium hydroxide and distilled. Dichloromethane was stored on calcium hydride, refluxed, and distilled. Precoated Macherey−Nagel Alugram SIL G/UV 254 plates were used for thin-layer chromatography (TLC) and the products were visualized with UV light. Column chromatography was performed on Acros Chimica silica gel (0.2−0.5 mm, pore size 4 nm).

N^6-Benzoyl-9-[(1*S*,4*R*,5*S*)-5-hydroxy-4-hydroxymethyl-2-cyclohexenyl]adenine (2). To a solution of **1** (500 mg, 1.67 mmol, dried three times with dry pyridine) in dry pyridine (20 mL) at 0 °C under nitrogen was added dropwise TMS−Cl (1.06 mL, 8.38 mmol, 5 eq). After the mixture was stirred for 1 h, BzCl (0.97 mL, 8.38 mmol, 5 eq) was added slowly. The reaction mixture was stirred for 1 h at 0 °C, warmed to room temperature, and stirred for additional 13 h. The reaction mixture was then cooled in an ice-bath and quenched with water (3 mL). After the mixture was stirred for 5 min, 25% NH_4OH solution (5 mL) was added. The resulting mixture was stirred at room temperature for 15 min and concentrated. The residue was dissolved in MeOH (15 mL) and 25% NH_4OH solution (10 mL) and stirred at room temperature for 0.5 h. After concentration, the residue was purified on silica gel (CH_2Cl_2-MeOH 50:1, 20:1, and 10:1) to afford **2** (385 mg, 63%) as white foams. ^{1}H NMR (DMSO-d_6) δ 2.01 (m, 1H), 2.15 (m, 2H), 3.60 (m, 2H), 3.78 (m, 1H), 4.76 (t, 1H, J = 5.1 Hz, −CH_2OH), 4.84 (d, 1H, J = 4.4 Hz, −CHO*H*), 5.42 (m, 1H), 5.88 (dm, 1H, J = 9.9 Hz), 6.05 (dm, 1H, J = 9.9 Hz), 7.59 (m, 3H), 8.04 (m, 2H), 8.34 (s, 1H), 8.76 (s, 1H), 11.17 (br-s, 1H, −NH); ^{13}C NMR (CD_3OD) δ 36.9 (t), 47.7 (d), 51.4 (d), 63.1 (t), 64.9 (d), 125.3 (d), 129.5 (d), 129.9 (d), 134.0 (d), 135.1 (s), 136.1 (d), 144.8 (d), 151.2 (s), 153.1 (d), 153.3 (s), 168.3 (s); UV λ_{max} (MeOH) = 280 nm; LISM (THGLY) 366 $(M + H)^+$; high-resolution mass spectrometry (HRMS) calcd for $C_{19}H_{20}N_5O_3$ $(M + H)^+$ 366.1566, found 366.1571.

N^6-Benzoyl-9-[(1*S*,4*R*,5*S*)-5-hydroxy-4-monomethoxytrityloxymethyl-2-cyclohexenyl]-adenine (3). To a solution of **2** (240 mg, 0.66 mmol, dried three times with dry pyridine) in dry pyridine (5 mL) at 0 °C under nitrogen was added MMTrCl (305 mg, 0.99 mmol, 1.5 eq) in portions. After the mixture was stirred at 0 °C for 0.5 h, the reaction was warmed to room temperature and kept at this temperature for 22 h. The reaction mixture was cooled in an ice bath and treated with MeOH (5 mL). After the mixture was stirred at room temperature for 0.5 h, the resulting mixture was concentrated. The residue was coevaporated with toluene to remove traces of pyridine and chromatographed on silica gel ($CHCl_3$-MeOH 100:1, 1% Et_3N) to afford **3** (240 mg, 57%) as white foam. ^{1}H NMR ($CDCl_3$) δ 2.12 (m, 2H), 2.54 (m, 1H), 3.24 (t, 1H, J = 8.8 Hz), 3.49 (s, 1H, −OH), 3.52 (dd, 1H, J = 8.8, 4.4 Hz), 3.78 (s, 3H), 3.85 (m, 1H), 5.43 (m, 1H), 5.82−5.96 (m, 2H), 6.84 (d, 2H, J = 7.8 Hz), 7.19−7.61 (m, 15H), 7.88 (s, 1H), 8.01 (d, 1H, J = 7.3 Hz), 8.75 (s, 1H), 9.35 (s, 1H, −NH); ^{13}C NMR ($CDCl_3$) δ 35.6 (t), 44.3 (q), 49.5 (d), 55.2 (d), 65.6 (t), 66.4 (d), 87.2 (s), 113.3 (d), 123.4 (s), 123.9 (d), 127.2 (d), 128.0 (d), 128.3 (d), 128.8 (d), 130.2 (d), 132.7 (d), 133.8 (s), 133.9 (d), 135.1 (s), 141.8 (d), 143.9 (s), 144.0 (s), 149.6 (s), 151.6 (s), 152.4 (d), 158.8 (s), 164.8 (s); UV λ_{max} (MeOH) = 280, 254 nm; LISMS (THGLY/NBA) 660 $(M + Na)^+$; HRMS calcd for $C_{39}H_{35}N_5O_4Na$ $(M + Na)^+$ 660.2587, found 660.2589.

Preparation of the Amidite Monomer 4. The modified nucleoside **3** (500 mg, 0.78 μmol), was phosphitylated with 2-cyanoethyl-*N*,*N*-diisopropyl-chlorophosphoramidite analogous to previous procedures.[8] Following column chromatography with *n*-hexane/acetone/triethylamine (58/40/2) and precipitation in cold hexane, an amount of 550 mg (0.66 μmol, 85%) of the amidite was isolated. R_f (*n*-hexane/acetone/triethylamine 49/49/2) 0.38 LSIMS (positive mode, NPOE) 838 $[M + H]^+$; ^{31}P NMR δ 148.51; ^{13}C NMR ($CDCl_3$, only relevant signals are given) δ 20.2 (CH_2), 24.4 (CH_3), 43.0, 43.2 (2xd, CH), 58.0, 58.5 (2xd, J = 18.8 Hz, $POCH_2$), 66.6, 68.2 (2xd, J = 17.5 Hz, C5′), 117.4 (CN) ppm.

Solid-Phase Oligonucleotide Synthesis. Assembly was done at a 1 μmol scale (10 μmol for the Dickerson sequence) on an ABI 381A DNA synthesizer following standard procedures[8] except for use of a 0.12 M solution of the unnatural amidite with a 3 min coupling time.

(28) Eschenmoser, A. *Proceedings Robert A. Welsch Foundation, 37th Conference on Chemical Research*; 1993; pp 201−235.

(29) De Winter, H.; Lescrinier, E.; Van Aerschot, A.; Herdewijn, P. *J. Am. Chem. Soc*. **1998**, *120*, 5381−5394.

Detritylation time for the monomethoxytrityl group was doubled. The ribooligonucleotides were assembled by Eurogentec.

Mass Spectrometry. Oligonucleotides were dissolved in water−acetonitrile (50:50) and desalted by means of Dowex-50W cation exchange beads. The supernatant was diluted by the addition of a 10-fold volume of water−acetonitrile−ammonia (50:50:0.3%). Electrospray MS and MS−MS data were acquired on a Micromass Q-Tof mass spectrometer (Whytenshawe, Manchester, UK) fitted with a nanospray ion source (ESI−MS) and operated in the negative mode. The instrument was calibrated with a two-point calibration using the singly charged ion of the monomer and dimer of raffinose.

CD Experiments. CD spectra were measured with a Jasco 600 spectropolarimeter in thermostatically controlled 1 cm cuvettes connected with a Lauda R CS 6 bath. The oligomers were dissolved and analyzed in a solution of NaCl (0.1 M) potassium phosphate buffer (20 mM), pH 7.5, EDTA 0.1 mM at 25 °C and at a concentration of 5 μM for each strand.

RNase H Experiment. The oligonucleotide 5′-CmGmGmCmGmrUrUrUrUrUCm AmGmGmAm-3′ was radiolabeled (^{32}P) at the 5′-end using T_4 polynucleotide kinase (Gibco BRL) and [γ-^{32}P]adenosine 5′-triphosphate (ATP) (4500 Ci/mmol, ICN) by standard procedures[30] and purified on a NAP-5 column (Pharmacia). The radiolabeled oligonucleotide (2.5 pmol) and the complementary oligonucleotide (50 nmol) with deoxy-, cyclohexene, or anhydrohexitol building blocks, respectively, were incubated in a total volume of 50 μL containing 10 mM Tris-chloride, pH 7.5, 25 mM KCl, and 0.5 mM $MgCl_2$ at 37 °C for 15 min, allowing the duplex to be formed. Cleavage reactions were started by the addition of 30 U RNase H (*E. coli* ribonuclease H, Amersham) to the mixture. Control tubes received no enzyme. Aliquots were taken at appropriate time intervals, mixed with an equal volume of stop mix (EDTA 50 mM, xylene cyanol FF 0.1%, and bromophenol blue 0.1% in formamide 90%) and chilled on ice. Samples were analyzed by denaturing 20% polyacrylamide gel electrophoresis (PAGE) containing urea (50%) with TBE buffer at 1000 V for 1.25 h. Results were visualized by phosphorimaging (Packard Cyclone, Optiquant software).

Enzymatic Stability. The oligonucleotides $(dA)_{13}$-propanediol, $(A_1)_{13}$-propanediol, and $(A_2)_{13}$-propanediol were radiolabeled (^{32}P) at the 5′-end using T_4 polynucleotide kinase (Gibco BRL) and [γ-^{32}P]-ATP (4500 Ci/mmol, ICN) by standard procedures and purified on a NAP-5 column (Pharmacia). To test for a broad range of enzymatic activity, 20 pmol radiolabeled oligonucleotide was incubated in 20 μL of 50% fetal calf serum in phosphate buffered saline (PBS) at 37 °C. Aliquots were taken at appropriate time intervals, mixed with a double volume of stop mix (EDTA 50 mM, xylene cyanol FF 0.1%, and bromophenol blue 0.1% in 7 M ureum), and chilled on ice. Samples were analyzed by denaturing 20% PAGE containing urea (50%) with TBE buffer at 1000 V for 1.25 h. Results were visualized by phosphorimaging (Packard Cyclone, Optiquant software).

UV Mixing Curve. Experiments were performed in a buffer containing 0.1 M NaCl, 0.02 M potassium phosphate pH 7.5, and 0.1 μM EDTA at 10 °C. The different samples were prepared by mixing 4 μM solutions of both strands, $(A_1)_{13}$ and dT_{13}, at the appropriate ratio. The samples were allowed to stabilize for 2 h, after which UV absorbance was measured with a Varian Cary 300 Bio spectrophotometer at 260 nm. The curve was obtained by means of linear regression.

NMR Sample Preparation and NMR Spectroscopy. NMR samples were prepared by dissolving the oligomer in 300 μL of NMR buffer which consisted of 0.1 M NaCl, 10 mM KH_2PO_4 and 10 μM EDTA, pH 7.5. The sample was lyophilized from 99.96% D_2O. The sample was finally dissolved in 300 μL 99.96% D_2O (or 90% H_2O and 10% D_2O for exchangeable proton NMR experiments). The samples were annealed by heating to 80 °C followed by slow cooling. The total concentration of the duplex was 1.4 mM.

NMR spectra were recorded on a Varian 500 unity spectrometer (operating at 499.505 MHz) using 3 mm triple resonance (HCP) probe. Quadrature detection was achieved by States−Haberkorn hypercomplex mode.[31] Spectra were processed using the programs NMRPipe[32] and XEASY[33] running on a Silicon Graphics O2 workstation (IRIX version 6.5).

Exchangeable proton NMR spectra of the sample dissolved in 90%H_2O/10%D_2O were recorded at 20 °C using WATERGATE pulse sequence.[11] Sweep widths of 12 000 Hz in both dimensions were used with 32 scans, 2048 data points in t_2 and 600 FIDs in t_1. The data were apodized with a shifted sine-bell square function in both dimensions and processed to a 4 K × 2 K matrix. The 2D DQF−COSY,[13] TOCSY,[14] and NOESY[12] spectra from the sample in D_2O were recorded at 20 °C with sweep widths of 5000 MHz in both dimensions. The residual HDO peak was suppressed by presaturation. The ^{31}P-decoupled (on resonance continuous decoupling) DQF−COSY spectrum consisted of 4096 datapoints in t_2 and 512 increments in t_1. The data were apodized with a shifted sine-bell square function in both dimensions and processed to a 4 K × 2 K matrix. For the TOCSY experiment, a Clean MLEV17[14] version was used with a TOCSY mixing time of 65 ms. The spectrum was acquired with 32 scans, 2048 data points in t_2, and 512 FIDs in t_1. The data were apodized with a shifted sine-bell square function in both dimensions and processed to a 4 K × 2 K matrix. The NOESY experiments were acquired with mixing times of 50, 100, 150, and 250 ms, 32 scans, 2048 datapoints in t_2, and 512 increments in t_1. A ^{1}H-^{31}P HETCOR[15] was acquired with 128 scans, 2048 datapoints in the proton dimension, t_2, and 512 real datapoints in the phosphorus dimension, t_1, over sweep widths of 5000 and 2000 Hz, respectively.

Model Building. The model building and conformational analysis of the CeNA monomer was done using Macromodel 5.0 as descibed previously.[34] The building and MD simulation of the polymer duplexes was done using midasplus and Amber 4.1.[29] The CeNA/RNA duplex was built starting from a 13-mer Arnott A-type double RNA helix (A/U base pairs). The CeNA/RNA duplex was built starting from a 13-mer Arnott B-type double-stranded DNA helix (A/T base pairs). The duplexes were soaked in a rectangular box of explicit TIP3P water molecules and 12 Na^+ counterions. After equilibration a 100 ps MD simulation was started (with particle mesh Ewald conditions) to verify the stability of the model structures.

Acknowledgment. We are grateful to Dr. Alan Millar (Micromass UK) and to Dr. Jan Claereboudt (Micromass Belgium) for providing us with the Q-Tof mass spectra. This research was supported by a grant for the K. U. Leuven (GOA 97/11). Arthur Van Aerschot is a research associate of the Flemish Fund of Scientific Research. Chris Hendrix is a fellow of the Rega Foundation. We thank Chantal Biernaux for editorial help.

Supporting Information Available: S1—Equilibrium between two-half-chair conformations of a cyclohexene nucleoside. S2—Top: ion exchange profile of the crude synthesis mixture for $(A_1)_{13}$. Conditions: Mono Q 5/5 column with NaCl gradient at pH 12 (0.01 M NaOH). Bottom: RP-HPLC analysis of the isolated material (Purospher STAR−RP-18 endcapped 3 μM, CH_3CN gradient in NH_4HCO_3 25 mM). S3—Serum stability (50% fetal calf serum in PBS) of oligoadenylates at 0, 5, 10, 30, 60, 180 min incubation time at 37 °C. (A) dA_{13}; (B) oligo-$(A_1)_{13}$; (C) oligo$(A_2)_{13}$. This material is available free of charge via the Internet at http:/pubs.acs.org. See any current masthead page for ordering information and Web access instructions.

JA000018+

(30) Maniatis, T.; Fritsch, E.; Sambrook, J. *Molecular Cloning*: *A Laboratory Manual*; Cold Spring Harbor Laboratory: New York, 1989.

(31) States, D. J.; Haberkorn, R. A.; Ruben, D. J. *J. Magn. Res.* **1982**, *48*, 286−292.

(32) Delaglio, F.; Grzesiek, S.; Vuister, G.; Zhu, G.; Pfeifer, J.; Bax, A. *J. Biomol. NMR* **1995**, *6*, 277−293.

(33) Xia, T.; Bartels, C. *Institute of Molecular Biology and Biophysics* 1994, Zürich, Switzerland.

(34) Ostrowski, T.; Wroblowski, B.; Busson, R.; Rozenski, J.; De Clercq, E.; Bennett, M. S.; Champness, J. N.; Summers, W. C.; Sanderson, M. R.; Herdewijn, P. *J. Med. Chem.* **1998**, *41*, 4343−4353.